

PS-wave polarity reversal in angle domain common-image gathers

Daniel Rosales and James Rickett, Geophysics Department, Stanford University

SUMMARY

The change in the wavelet polarity at near offsets is a fundamental feature of converted wave seismology due the vector-nature of the displacement field. The conventional way of dealing with this feature is to reverse the polarity of data recorded at negative offsets. This process can have some problems in presence of structural complexity. Angle domain common-image gathers (CIGs) map the seismic energy with respect to the reflection angle; this mapping property leads to a clear strategy for correctly handling the polarity reversal after pre-stack migration for arbitrarily complex earth models. Results on synthetic data illustrate one of the advantages of working with converted waves in angle domain CIGs: handle the polarity flip correctly.

INTRODUCTION

An important issue in converted wave seismic processing is how to deal with the polarity reversal that occurs near zero-offset. Conventional methodology (Harrison and Stewart, 1993) involves multiplying the data recorded at negative offsets by -1 . However, this approach fails where there is structural complexity and non-constant γ ($= v_p/v_s$).

For P -wave datasets, angle-domain common-image gathers [e.g. de Bruin et al. (1991); Prucha et al. (1999)] decompose reflected seismic energy into components from specific opening angles (θ). Since the PS -wave polarity reversal occurs at normal incidence ($\theta = 0$), the angle-domain common-image gathers provide a natural domain in which to address the problem. Moreover, analyzing angle gathers for converted wave seismic data may lead to other new technologies that can take advantage of this domain: for example, velocity analysis and amplitude versus angle analysis.

In this work we present a theoretical discussion of the polarity reversal problem. We image PS -wave data into offset-domain CIGs with a prestack finite-frequency recursive depth migration algorithm. We then use the radial-trace transformation introduced by Sava and Fomel (2000) in order to obtain angle-domain gathers after migration. A simple reinterpretation of the opening angle (θ) for the case of converted waves leads to a solution to the polarity reversal problem that is valid for dipping events in areas with complex velocity.

THEORY

Polarity flip

The polarity inversion visible at near-offsets in converted wave data is an intrinsic property of the shear wave displacement. In a constant velocity medium, the vector displacement field produces opposite movements in the two geophones either side of zero-offset. This leads to the polarity flip in the seismic gather (Figure 1).

For more complex velocities, the normal incidence ray determines the location of the polarity flip. For flat reflectors in $v(z)$ media, or in areas with constant γ , the normal incidence ray will emerge at the surface at zero-offset. However, in general, the P and S -wave ray paths corresponding to the normal-incidence (zero-amplitude) ray will not necessarily emerge at the surface at the same point. Figure 2 illustrates this for the case of a dipping layer and a non-constant γ .

This path deviation produces a polarity reversal at non-zero

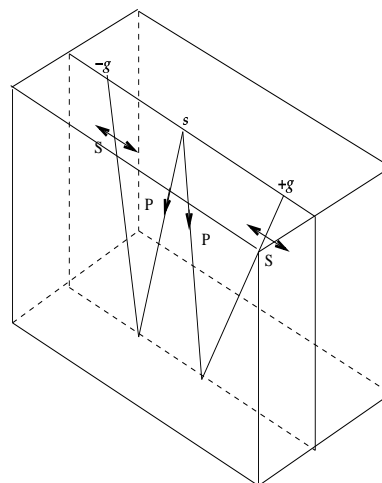


Figure 1: Polarity inversion in converted waves seismic data. $+g$ and $-g$ correspond to positive and negative polarity in a common shot gather. Modified from Tatham and McCormack (1991).

offset in the data space. In areas of complex structure, the picking of this polarity flip point is difficult; however, in the angle domain (model space), this point is a uniquely determined function of the P -velocity, S -velocity, and reflector dip; therefore, it is easy to correct the polarity flip in the model space.

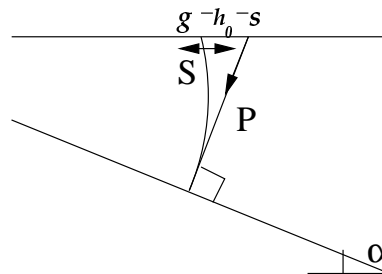


Figure 2: Polarity flip problem for a dipping layer and a non-constant γ .

Converted-wave migration by depth extrapolation

Recursive migration methods based on wavefield extrapolation have the advantage over Kirchhoff methods in that they accurately handle the finite-frequency effects of wave-propagation. For example, rough velocity models and triplating wavefronts that can cause problems for Kirchhoff migrations present no difficulties for recursive methods. Biondi and Vaillant (2000) demonstrated these advantages for a complex 3-D P -wave dataset.

For the examples in this paper, we migrated the prestack data with a shot-profile migration algorithm, imaging the cross-correlation of upgoing and downgoing wavefields at zero-time

(Claerbout, 1971); however, the methodology is also applicable for “survey-sinking” shot-geophone algorithms based on the double square root equation (Claerbout, 1985).

Migrating converted waves with conventional wavefield extrapolation algorithms simply involves extrapolating downgoing waves with the P -wave velocity field, and upgoing waves with the S -wave velocity field. The difficulty comes in the interpretation of common-image gathers in terms of incidence angle at the reflector.

Angle domain common image gathers

Both de Bruin et al. (1991) and Prucha et al. (1999) obtain P -wave angle-domain common-image gathers by slant-stacking the wavefields during migration, before invoking the imaging condition. Their methodologies suit shot-profile and shot-geophone algorithms, respectively. However, we follow an alternative approach advocated by Sava and Fomel (2000).

Fomel (1996) derived the partial differential equation describing the image surface in a depth-midpoint-offset space:

$$\tan \theta = - \left. \frac{\partial z}{\partial h} \right|_{t,x}, \quad (1)$$

where θ is the P -wave opening or incidence angle. Unfortunately, θ has a more complex meaning for PS -seismic. In this case, the angle relates the P -incidence angle, the S -reflection angle, and the structural dip, α .

This paper presents a simplification of the problem of common angle gathers for converted waves, which is the determination of the polarity flip in the angle domain. We define θ_0 as the *polarity flip angle*, for which the P -incidence angle equals the S -reflection angle, and they are both equal to zero, i.e. normal incidence. Thus θ_0 corresponds to the point of polarity flip in angle domain. Equation (2) gives θ_0 as a function of the structural dip, P -velocity, and S -velocity.

$$\tan \theta_0 = \frac{v_p - v_s}{v_p + v_s} \tan \alpha. \quad (2)$$

Methodology

The polarity flip angle depends on both velocity fields and on the layer's dip. Its determination is of crucial importance for the polarity regularization. This section describes the basic steps of our methodology for the polarity flip angle determination and polarity regularization. The algorithm that we use is:

1. Common shot depth migration to offset-domain CIGs.
2. Transform offset-domain gathers into angle-domain gathers with equation (3).
3. Determine the polarity flip angle, θ_0 with equation (2).
4. Flip negative polarities in the angle domain.
5. Stack over angle to produce a final structural image.

The first step is to transform the data to the temporal frequency domain; subsequently, we downward continue the shot and receiver wavefields with v_p and v_s respectively, and image the data at zero time. In this way, we obtain the offset-domain CIGs, and if we use the correct velocity models, the energy is focused close to zero offset.

The common angle gathers are evaluated in the Fourier-domain by equation (3). The method involves a radial-trace mapping after migration in the k_h - k_z domain (Sava and Fomel, 2000). Rickett and Sava (2001) describe how we prepare the offset-domain CIGs with a shot-profile migration algorithm.

$$\tan \theta = - \frac{|\vec{k}_h|}{k_z}. \quad (3)$$

To determine the structural dip, we apply plane-wave destructors (Fomel, 2000), which characterize the seismic images as a superposition of local plane waves. With the dip field and the two migration velocity models, we calculate the polarity flip angle using equation (2). The polarity flip is an easy process after we have the polarity flip angle, we just apply a mask to the common angle gathers that follows the polarity flip angles and multiply the data by -1 .

NUMERICAL EXAMPLES

To test the methodology we created a realistic synthetic example. The model consists of five reflectors, dipping at angles of 0° , 15° , 30° , 45° , 60° , embedded in simple linear $v(z)$ velocities.

The velocity gradients were chosen in order to simulate a typical near seafloor velocity profile: the P -velocity model consists of an initial velocity of 1700 m/s and a gradient of 0.15 s^{-1} . On the other hand, the S -velocity model has an initial velocity of 300 m/s and a gradient of 0.35 s^{-1} .

We used ray-tracing in order to generate the data set. Figure 3 shows a common shot gather located in the center of the model. It is possible to note that the polarity flip varies with respect to the travel time as a function of the reflector dip and the $\frac{v_p}{v_s}$ ratio (Figure 2).

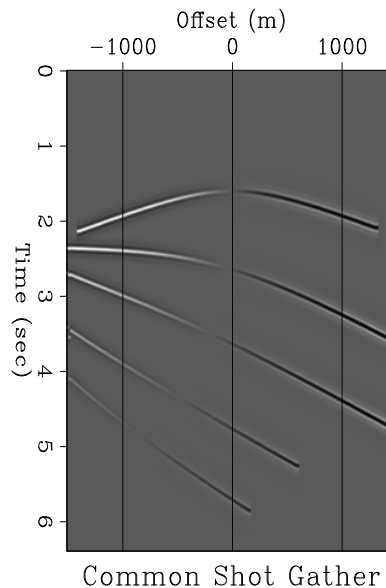


Figure 3: Common Shot Gather, taken in the middle of model.

Figure 4 shows an angle-domain gather after (left) and before (right) the polarity correction in the angle domain. It is possible to observe that the events in the common angle gathers are flat, which implies that we used the correct velocity model for the migration; moreover, it is possible to observe

in the common angle gather before the correction that the same event changes its polarity. The point for this change is the polarity flip angle (θ_0) determined by equation (2). With the P and S velocity models used for the migration and the dip map estimated by plane-wave destructors, we calculate the curve superimposed on the common angle gather, this curve represents the polarity flip angle. The angle-domain gather after the correction for the polarity inversion is in the right of Figure 4. It is clear that our methodology correctly handles the polarities after migration.

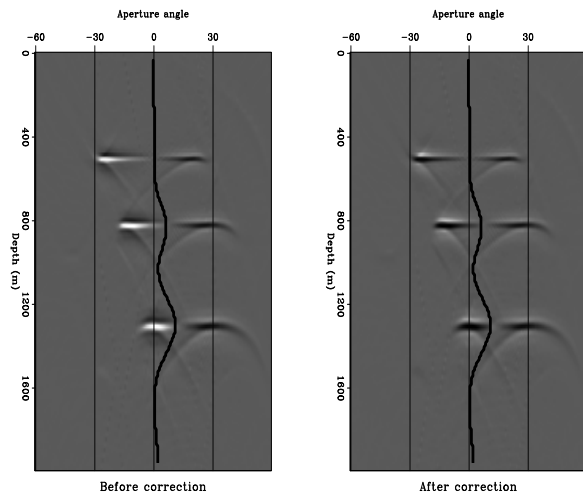


Figure 4: Common Angle Gather, After the pre-stack migration without the polarity correction (left). Before the pre-stack migration with the polarity correction (right). The line in the gather mark the polarity flip angle, as a function of the dip, P -velocity and S -velocity

Figure 5 presents the final migration results. The top represents the result with the correction in the data space and the bottom represents the result with the correction in the model space. With the correction after migration we can see that we recover perfectly all our events, note that for the steeply dipping events the correction in the model space recovers the events better than the correction in the data space.

CONCLUSIONS

We showed a series of important concepts in non-conventional PS -seismic processing for an important problem in converted wave seismic processing: the polarity flip.

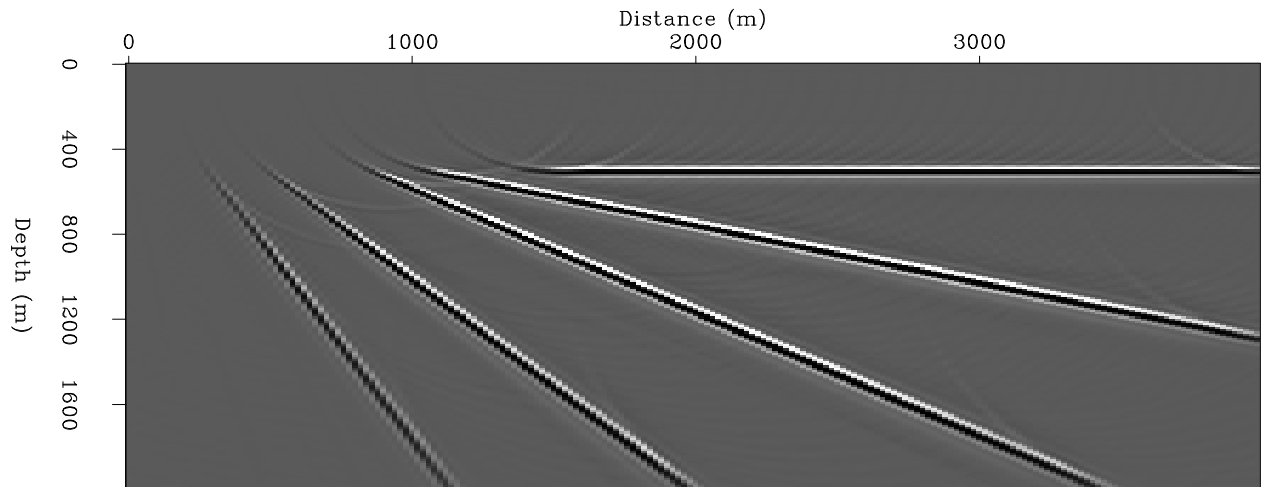
We used frequency domain common shot migration in order to obtain an image of the subsurface with converted waves data. The shot-profile migration algorithm enables the use of two different velocity models, one for the P -data and the other for the S portion of the data; therefore, we do not have to introduce a mixed PS -velocity model.

We introduce common angle gather for converted waves. In this domain the normal incidence reflection is determined by the polarity flip angle, this polarity flip angle helps to regularize the polarities in the angle domain, hence, in the seismic reflection data.

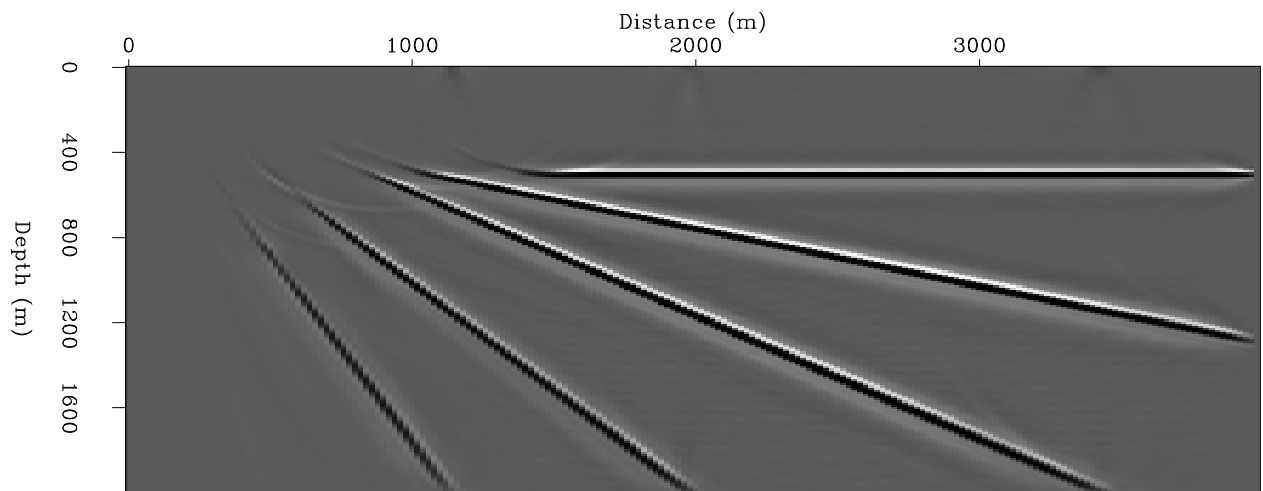
The introduction of common angle gather in converted waves seismic processing and imaging brings a series of opportunities for building S -velocity models, amplitude analysis versus angle for converted waves; therefore, the opportunity to extract as much extra information as possible from PS seismic data.

REFERENCES

- Biondi, B., and Vaillant, L., 2000, 3-d wave-equation prestack imaging under salt: 70th Ann. Internat. Meeting, Soc. Expl. Geophys., Expanded Abstracts, submitted.
- Claerbout, J. F., 1971, Toward a unified theory of reflector mapping: *Geophysics*, **36**, no. 3, 467–481.
- Claerbout, J. F., 1985, *Imaging the earth's interior*: Blackwell Scientific Publications, Inc.
- de Bruin, C. G. M., Wapenaar, C. P. A., and Berkhout, A. J., 1991, Angle-dependent reflectivity by means of prestack migration: *Geophysics*, **55**, no. 9, 1223–1234.
- Fomel, S., 1996, Migration and velocity analysis by velocity continuation: *SEP-92*, 159–188.
- Fomel, S., 2000, Applications of plane-wave destructor filters: *SEP-105*, 1–26.
- Harrison, M. P., and Stewart, R. R., 1993, Poststack migration of p-sv seismic data: *Geophysics*, **58**, no. 8, 1127–1135.
- Prucha, M., Biondi, B., and Symes, W., 1999, Angle-domain common image gathers by wave-equation migration: 69th Annual Internat. Mtg., Soc. Expl. Geophys., Society Of Exploration Geophysicists, Expanded Abstracts, 824–827.
- Rickett, J., and Sava, P., 2001, Offset and angle domain common image gathers for shot-profile migration: 71st Annual Internat. Mtg., Soc. Expl. Geophys., Society Of Exploration Geophysicists, submitted.
- Sava, P., and Fomel, S., 2000, Migration angle-gathers by Fourier Transform: *Geophysical Prospecting*, submitted.
- Tatham, R. H., and McCormack, M. D., 1991, Multicomponent seismology in petroleum exploration: Society Of Exploration Geophysicists.



Correction in the data space



Correction in the model space

Figure 5: Final Migration Section: The top figure shows the image with the polarity correction in the data space. The bottom figure shows the image with the polarity correction in the model space